

Palm calculus for stationary Cox processes on iterated random tessellations

Florian Voss, Catherine Gloaguen,*Member, IEEE*, and Volker Schmidt

Abstract—We investigate Cox processes of random point patterns in the Euclidean plane, which are located on the edges of random geometric graphs. Such Cox processes have applications in the performance analysis and strategic planning of both wireless and wired telecommunication networks. They simultaneously allow to represent the underlying infrastructure of the network together with the locations of network components. In particular, we analyze the Palm version X^* of stationary Cox processes X living on random graphs that are built by the edges of an iterated random tessellation T . We derive a representation formula for the Palm version T^* of T which includes the initial tessellation T_0 and the component tessellation T_1 of T as well as their Palm versions T_0^* and T_1^* . Using this formula, we are able to construct a simulation algorithm for X^* if both T_0, T_1 and their Palm versions T_0^*, T_1^* can be simulated. This algorithm for X^* extends earlier results for Cox processes on simpler (non-iterated) tessellations. It can be used, for example, in order to estimate the probability densities of various connection distances, which are important performance characteristics of telecommunication networks. In a numerical study we consider the particular case that T_0 is a Poisson-Voronoi tessellation and T_1 is a Poisson line tessellation.

Index Terms—Point processes, Geometric modeling, Poisson processes, Monte Carlo methods, Estimation, Mobile communication, Networks.

I. INTRODUCTION

Real telecommunication networks are huge and complex systems. They are deployed in a variety of settings (rural areas, towns, indoor...) and are built on technologies that depend on the users needs and specificities. Networking studies aim to find the best possible solutions to serve the requirements of customers under feasibility and cost constraints for the telecommunication operator, the latter being enhanced by the present context of market competition. Appropriate analysis tools are thus needed to relate possible network architecture and characteristics as well as traffic demand and variability to such notions as quality of service perceived by the users.

In particular, reliable and efficient tools are needed for the global analysis of huge networks that explicitly take into account the geometry of the territory while being able to describe various technologies and architectures. However, it is often impossible to do the analysis directly on real network data, e.g., due to the enormous size and complexity of modern telecommunication networks. A methodological

solution of this problem is to look at the complexity of the network from a macroscopic perspective. This can be achieved in the framework of stochastic modeling. Spatial stochastic modeling is a powerful approach for the purpose of global analysis of huge networks since it provides direct access to the statistical properties of the system. The main principles that govern the behavior of the network to be studied are translated via the choice of suitable random processes. They have been proved to be useful in order to describe the geometry of the underlying infrastructure or the locations of network components. Since the first applications of these tools to global network modeling, see e.g. [1]–[6], the variety of suitable spatial network models has been greatly enriched using concepts from stochastic geometry, like spatial point processes and random geometric graphs [7]–[9]. Traditionally, the locations of network components have been described by planar Poisson processes. The advantage of this approach is that the resulting network models are analytically tractable to a great extent. Unfortunately, this is not possible from end to end for most of the random processes involved in more realistic models, even under stationarity assumptions. However, planar Poisson processes represent the situation of complete spatial randomness and, therefore, seem to be inappropriate in many applications. For instance, in this way, geographical features of the considered region where a new network has to be deployed cannot be taken into account.

We regard more general classes of point processes which are able to include geographical features into the network model. In particular, we consider Cox processes located on the edges of random geometric graphs. Such processes can be used in order to model, e.g., the street system inside cities together with network components located along the streets [10]–[13]. We focus on random graphs which are constructed by the edges of random tessellations, whose distributions depend on a few parameters only. Anyhow, it turns out that by such tessellation models we are able to fit basic statistical properties of real street systems like the mean number of crossings, segments, city blocks and the mean total length of streets all measured per unit area. This means, for a given set of street data, it is possible to choose an optimal tessellation type and its parameters by the fitting techniques introduced in [14], [15].

We emphasize that this kind of Cox processes can be applied in the analysis of both wireless and wired telecommunication networks. For fixed access networks, parametric distance distributions of point-to-point connection distances along the edges of random tessellations were obtained using Palm calculus and efficient simulation algorithms for the typical cell [11], [16]. Note that the parameters of these

This work was supported by Orange Labs (Research agreement 46143714)

F. Voss and V. Schmidt are with the Institute of Stochastics, Ulm University, Helmholtzstraße 18, 89069 Ulm, Germany. E-mail: {florian.voss, volker.schmidt}@uni-ulm.de

C. Gloaguen is with Orange Labs, 38-40 rue du Général Leclerc, 92131 Issy-les-Moulineaux, France. E-mail: catherine.gloaguen@orange-ftgroup.com

distributions explicitly depend on the considered tessellation model. The parametric distance distributions for the optimal tessellation model were then compared to the corresponding distributions which were estimated from real data. Although the choice of the optimal tessellation model was restricted to simple tessellations of Poisson type, the distance distributions computed in [11] from the model and from real data, respectively, were already very close. Since the spatial distribution of the transmitters, receivers and relaying nodes is an essential feature for assessing the performance of wireless networks, we think that such an approach, although developed for fixed network analysis, could also be used in the framework of wireless and mobile networks. The aim of this paper is to make the reader aware of the possibility to include the geometry of road systems in wireless network analysis. For example, the distributions of direct (Euclidean) connection distances can be computed for network components located along street systems and belonging to different hierarchy levels of the network [12].

In [14] we showed that iterated tessellations [17], [18] lead to much better fits regarding the underlying street system than simple (non-iterated) tessellations of Poisson type. Thus, we also expect even better results for the fitting of distance distributions than those obtained in [11]. In the present paper, we therefore extend some results, which we recently derived for stationary Cox processes on simple (non-iterated) tessellations of Poisson type, to Cox processes X concentrated on iterated tessellations T . Note that T is then built by an initial tessellation T_0 and a component tessellation T_1 . For the analysis of cost functionals like the distributions of connection distances, it is fundamental to analyze the Palm version X^* of the Cox process X . Unfortunately, it is often impossible to get closed analytical expressions for the distribution of X^* . However, alternatively, simulation algorithms for X^* can be used in order to analyze various performance characteristics of the network. For example, in hierarchical network models it is possible to estimate distance distributions in an efficient way based on samples of the typical Voronoi cell of X which can be constructed from X^* , see e.g. [10], [12].

In Theorem 3.1, we derive a representation formula for the distribution of the Palm version T^* of T which includes the initial tessellation T_0 and the component tessellation T_1 of T as well as their Palm versions T_0^* and T_1^* . Using this formula, we are able to construct a simulation algorithm for X^* if both T_0, T_1 and their Palm versions T_0^*, T_1^* can be simulated. This algorithm for X^* extends earlier results for Cox processes on simpler (non-iterated) tessellations of Poisson type. Note that so far simulation algorithms for X^* were available only for Cox processes on Poisson-Delaunay tessellations (PDT), Poisson-Voronoi tessellations (PVT), and Poisson line tessellations (PLT), respectively [12], [19], [20]. Other extensions are also possible, e.g., to Cox processes on modulated Poisson-Voronoi tessellations [21] which yield a suitable model for nationwide networks.

The paper is organized in the following way. First, in Section II, we briefly explain some mathematical background, introducing the notion of iterated random tessellations T and defining Cox processes X on their edge set ∂T . Subsequently,

in Section III, we derive a representation formula for the distribution of the Palm version T^* of T . Based on this formula we introduce a new simulation algorithm for X^* . Finally, in Section IV, we demonstrate in a numerical study how our results can be used in order to estimate the density of various distance distributions based on the typical Voronoi cell of X .

II. COX PROCESSES ON ITERATED TESSELLATIONS

In this section we describe the kind of tessellation and point-process models for wireless and wired telecommunication networks, which we consider in the present paper. Moreover, we briefly explain some necessary mathematical background and notation. Comprehensive surveys on the usage of stochastic geometry and random geometric graphs in spatial modeling of telecommunication networks can be found in [7]–[9]. For further details on point processes and random tessellations see e.g. [22]–[25].

A. Iterated tessellations

A (planar) random tessellation T is a subdivision of \mathbb{R}^2 into a sequence Ξ_1, Ξ_2, \dots of random compact and convex polygons, which are not overlapping and locally finite, i.e., $\bigcup_{i=1}^{\infty} \Xi_i = \mathbb{R}^2$, $\text{int} \Xi_i \cap \text{int} \Xi_j = \emptyset$ for $i \neq j$, and $\#\{i : \Xi_i \cap B \neq \emptyset\} < \infty$ for each bounded set $B \subset \mathbb{R}^2$. Note that T can be identified with its edge set $\partial T = \bigcup_{n=1}^{\infty} \partial \Xi_n$. Furthermore, we need the notion of an iterated tessellation (or, equivalently, nested tessellation), where we consider some initial tessellation T_0 and a sequence T_1, T_2, \dots of independent component tessellations, which are independent of T_0 . Then, for each $n \geq 1$, the n th cell Ξ_{0n} of T_0 is considered together with its „inner structure“ $\Xi_{0n} \cap \partial T_n$, where the intersection $\Xi_{0n} \cap \partial T_n$ means that part of the edge system ∂T_n of T_n which is contained in the cell Ξ_{0n} of T_0 . The edge set of the iterated tessellation T is then defined by $\partial T = \bigcup_{n=1}^{\infty} \partial \Xi_{0n} \cup (\Xi_{0n} \cap \partial T_n)$. A realization of an iterated tessellation is shown in Fig. 1. In particular, by Ξ_{01} we denote the so-called zero cell of T_0 , i.e., that cell of T_0 containing the origin, where the inner structure of Ξ_{01} is given by $\Xi_{01} \cap \partial T_1$. For brevity, we write $T = \tau(T_0 | T_1, T_2, \dots)$ for an iterated tessellation induced by T_0 and T_1, T_2, \dots . Note that $T = \tau(T_0 | T_1, T_2, \dots)$ is stationary if T_0 is stationary and if T_1, T_2, \dots are identically distributed and stationary. Then, by $\gamma_0 = \mathbb{E}\nu_1(\partial T_0 \cap [0, 1]^2)$ and $\gamma_1 = \mathbb{E}\nu_1(\partial T_1 \cap [0, 1]^2)$ we denote the intensities of T_0 and T_1 , respectively, where ν_1 is the one-dimensional Hausdorff measure in \mathbb{R}^2 . Moreover, the intensity $\gamma = \mathbb{E}\nu_1(\partial T \cap [0, 1]^2)$ of T is given by $\gamma = \gamma_0 + \gamma_1$.

B. Cox processes

Let T_0, T_1, T_2, \dots be independent stationary tessellations, where T_1, T_2, \dots are identically distributed, but the distribution of T_0 can be different from that of T_1, T_2, \dots . In the following we assume that the point process $X = \{X_n\}$ is a stationary Cox process in \mathbb{R}^2 with random intensity measure Λ given by $\Lambda(B) = \lambda_\ell \nu_1(\partial T \cap B)$ for each Borel set $B \subset \mathbb{R}^2$ and some $\lambda_\ell > 0$, where $T = \tau(T_0 | T_1, T_2, \dots)$. Note that given T the points X_1, X_2, \dots of X are then placed as

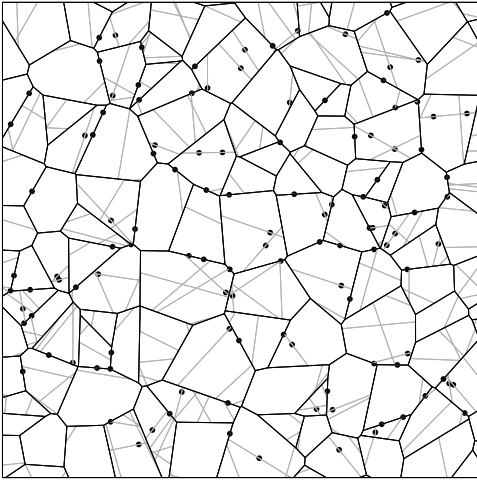


Fig. 1. Cox process (black points) on an iterated tessellation with PVT (black) and PLT (Grey) as T_0 and T_1

linear Poisson processes on the edges of T . Furthermore, the (planar) intensity $\lambda = \mathbb{E}\#\{n : X_n \in [0, 1]^2\}$ of X is given by $\lambda = \lambda_\ell \gamma$, where γ is the intensity of T and λ_ℓ can be interpreted as the (linear) intensity of the conditional Poisson processes on the edges of T . A realization of a Cox process together with the underlying iterated tessellation is displayed in Fig. 1.

C. Scaling invariance and scaling limits

Recall that the intensities of T_0 and T_1 are denoted by γ_0 and γ_1 , respectively. If we scale T by a constant $c > 0$, then $cT \stackrel{d}{=} T'$, where T' is an iterated tessellation with initial tessellation T'_0 and component tessellation T'_1 such that $T'_0 \stackrel{d}{=} cT_0$ and $T'_1 \stackrel{d}{=} cT_1$. The intensities γ'_0 and γ'_1 of T'_0 and T'_1 are given by $\gamma'_0 = \gamma_0/c$ and $\gamma'_1 = \gamma_1/c$, respectively.

If X is a Cox process on T with linear intensity λ_ℓ and X' is a Cox process on T' with linear intensity $\lambda'_\ell = \lambda_\ell/c$, then $cX \stackrel{d}{=} X'$. Thus, if $\gamma_0/\gamma_1 = \gamma'_0/\gamma'_1$ and if the scaling factors $\kappa = \gamma/\lambda_\ell$ and $\kappa' = \gamma'/\lambda'_\ell$ coincide, where $\gamma = \gamma_0 + \gamma_1$ and $\gamma' = \gamma'_0 + \gamma'_1$, then the Cox processes X and X' have the same distributions up to a scaling. This observation can be used in order to do numerical computations only for a single parameter triplet $(\gamma_0, \gamma_1, \lambda_\ell)$ with given ratio γ_0/γ_1 and scaling factor $\kappa = (\gamma_0 + \gamma_1)/\lambda_\ell$. For other parameter triplets $(\gamma'_0, \gamma'_1, \lambda'_\ell)$ with the same scaling factor κ and with $\gamma_0/\gamma_1 = \gamma'_0/\gamma'_1$ we can then obtain the corresponding results from the already computed ones by an appropriate scaling, see [15]. Thus, in our numerical computations, we fix $\gamma = 1$ and only vary $\gamma_0 \in [0, 1]$ and $\lambda_\ell > 0$, where $\gamma_1 = 1 - \gamma_0$, see Sections IV.

Furthermore, the following convergence results can be proved. On the one hand, one can show that X converges weakly to a (planar) Poisson process with intensity λ if $\kappa \rightarrow \infty$ and $\lambda_\ell \gamma (= \lambda)$ is fixed. Thus, it is interesting to compare numerical results for Cox processes on T to corresponding results for Poisson processes with the same intensity. On the other hand, one can show that T converges weakly to T_0 and T_1 if $\gamma_1 \rightarrow 0$ and $\gamma_0 \rightarrow 0$, respectively. Thus, we can compare numerical results for Cox processes on iterated tessellations

to corresponding results for Cox processes on simpler (non-iterated) tessellations.

III. PALM DISTRIBUTIONS

In this section we consider the Palm version of the stationary Cox process X , which is a point process X^* in \mathbb{R}^2 whose distribution is given by

$$\mathbb{E}h(X^*) = \frac{1}{\lambda} \mathbb{E} \sum_{i: X_i \in [0, 1]^2} h(\{X_n\} - X_i), \quad (\text{III.1})$$

where $h : \mathbb{N} \rightarrow [0, \infty)$ is an arbitrary measurable function and \mathbb{N} denotes the family of all locally finite sets $\{x_n\} \subset \mathbb{R}^2$. Note that $\mathbb{P}(o \in X^*) = 1$ by definition, where the distribution of X^* is called the Palm distribution of X . It can be interpreted as conditional distribution of X given that there is a point at the origin. Furthermore, it can be shown that the so-called reduced Palm version $X^* \setminus \{o\}$ of X is a Cox process, too. The random intensity measure Λ^* of $X^* \setminus \{o\}$ is given by $\Lambda^*(B) = \lambda_\ell \nu_1(\partial T^* \cap B)$ for each Borel set $B \subset \mathbb{R}^2$, where T^* is a random tessellation whose distribution is given by

$$\mathbb{E}h(T^*) = \frac{1}{\gamma} \mathbb{E} \int_{T \cap [0, 1]^2} h(T - x) \nu_1(dx), \quad (\text{III.2})$$

where $h : \mathbb{T} \rightarrow [0, \infty)$ is an arbitrary measurable function and \mathbb{T} denotes the family of all tessellations in \mathbb{R}^2 . Note that $\mathbb{P}(o \in \partial T^*) = 1$ by definition, where the distribution of T^* is called the Palm distribution of T . It can be interpreted as conditional distribution of T given that the origin belongs to an edge of T .

Palm distributions are important objects in the analysis of telecommunication networks. For instance, we can associate to each point X_n of X its Voronoi cell Ξ_n . If we assume that X_n represents a network component, then Ξ_n can be regarded as the domain it has to serve. The typical Voronoi cell of X_n is then defined as the Voronoi cell at the origin with respect to X^* . Note that the distribution of the typical cell can be regarded as the limit of the empirical distributions of all Voronoi cells in a family of unboundedly increasing sampling windows.

A. Representation formula for T^*

Assume that the random intensity measure Λ of the stationary Cox process X is the one-dimensional Hausdorff measure concentrated on the edge set ∂T of a (stationary) iterated tessellation $T = \tau(T_0 \mid T_1, T_2, \dots)$, where T_0, T_1, T_2, \dots are independent stationary tessellations and T_1, T_2, \dots are identically distributed.

In Section III-B we present a simulation algorithm for the typical Voronoi cell of X , or, equivalently, for the Voronoi cell of X^* with respect to the origin. This algorithm is based on the following representation formula for T^* , which includes the Palm versions T_0^* and T_1^* of T_0 and T_1 , respectively. In particular, the iterated tessellations $\tau(T_0^* \mid T_1, T_2, \dots)$ and $\tau(T_0 \mid T_1^*, T_2, T_3, \dots)$ are considered, where, in the latter case, the zero-cell Ξ_{01} of T_0 has the component tessellation T_1^* , and the other cells of T_0 have the component tessellations T_2, T_3, \dots , respectively.

Theorem 3.1: For any measurable function $h : \mathbb{T} \mapsto [0, \infty)$, it holds that

$$\begin{aligned} \mathbb{E}h(T^*) &= \frac{\gamma_0}{\gamma} \mathbb{E}h(\tau(T_0^* | T_1, T_2, \dots)) \\ &\quad + \frac{\gamma_1}{\gamma} \mathbb{E}h(\tau(T_0 | T_1^*, T_2, T_3, \dots)). \quad (\text{III.3}) \end{aligned}$$

Proof: Using (III.2), we can write $\mathbb{E}h(T^*)$ as

$$\begin{aligned} \mathbb{E}h(T^*) &= \frac{1}{\gamma} \mathbb{E} \left[\int_{T \cap [0,1]^2} h(T-x) \nu_1(dx) \right] \\ &= \frac{\gamma_0}{\gamma} \left(\frac{1}{\gamma_0} \mathbb{E} \left[\int_{T_0 \cap [0,1]^2} h(T-x) \nu_1(dx) \right] \right) \\ &\quad + \frac{\gamma_1}{\gamma} \left(\frac{1}{\gamma_1} \mathbb{E} \left[\sum_{i=1}^{\infty} \int_{T_i \cap \Xi_{0i} \cap [0,1]^2} h(T-x) \nu_1(dx) \right] \right), \end{aligned}$$

where $\Xi_{01}, \Xi_{02}, \dots$ are the cells of T_0 . Furthermore, we get that

$$\begin{aligned} &\frac{1}{\gamma_0} \mathbb{E} \left[\int_{T_0 \cap [0,1]^2} h(T-x) \nu_1(dx) \right] \\ &= \frac{1}{\gamma_0} \mathbb{E} \left[\int_{T_0 \cap [0,1]^2} h(\tau(T_0-x | T_1-x, T_2-x, \dots)) \nu_1(dx) \right] \\ &= \frac{1}{\gamma_0} \mathbb{E} \left[\int_{T_0 \cap [0,1]^2} h(\tau(T_0-x | T_1, T_2, \dots)) \nu_1(dx) \right] \\ &= \mathbb{E}h(\tau(T_0^* | T_1, T_2, \dots)). \end{aligned}$$

Note that the independence and stationarity of T_0, T_1, T_2, \dots have been used in the last but one equality, whereas the last equality is obtained from (III.2), replacing T and T^* by T_0 and T_0^* , respectively. It remains to show that

$$\mathbb{E}h(\tau(T_0 | T_1^*, T_2, T_3, \dots)) = \frac{1}{\gamma_1} \mathbb{E} \left[\sum_{i=1}^{\infty} \int_{T_i \cap \Xi_{0i} \cap [0,1]^2} h(T-x) \nu_1(dx) \right]. \quad (\text{III.4})$$

In the following we write \mathbb{E}_{T_i} , \mathbb{E}_{T_0, T_i} and $\mathbb{E}_{\{T_j\}}$ to indicate that the expectation is taken with respect to a single tessellation T_i , two tessellations T_0 and T_i , or an infinite sequence of tessellations $\{T_j\}$, respectively. Since T_0, T_1, T_2, \dots are independent and stationary, we get that

$$\begin{aligned} &\mathbb{E} \left[\sum_{i=1}^{\infty} \int_{T_i \cap \Xi_{0i} \cap [0,1]^2} h(T-x) \nu_1(dx) \right] \\ &= \sum_{i=1}^{\infty} \mathbb{E}_{T_0, T_i} \left[\int_{T_i \cap [0,1]^2} \mathbb{E}_{\{T_j\}_{j \neq i}} \left[\mathbb{I}_{\Xi_{0i}}(x) h(\tau(T_0-x | \{T_j-x\})) \right] \nu_1(dx) \right] \\ &= \sum_{i=1}^{\infty} \mathbb{E} \left[\int_{T_1 \cap [0,1]^2} \mathbb{I}_{\Xi_{0i-x}}(o) h(\tau(T_0-x | T_1-x, \{T_j\}_{j \geq 2})) \nu_1(dx) \right], \end{aligned}$$

where in the last expression $T_1 - x$ denotes the component tessellation which subdivides the zero cell of $T_0 - x$ for each $x \in \Xi_{0i}$. Furthermore, we have

$$\begin{aligned} &\sum_{i=1}^{\infty} \mathbb{E} \left[\int_{T_1 \cap [0,1]^2} \mathbb{I}_{\Xi_{0i-x}}(o) h(\tau(T_0-x | T_1-x, \{T_j\}_{j \geq 2})) \nu_1(dx) \right] \\ &= \mathbb{E} \left[\int_{T_1 \cap [0,1]^2} \sum_{i=1}^{\infty} \mathbb{I}_{\Xi_{0i}}(x) h(\tau(T_0-x | T_1-x, \{T_j\}_{j \geq 2})) \nu_1(dx) \right] \\ &= \mathbb{E} \left[\int_{T_1 \cap [0,1]^2} h(\tau(T_0-x | T_1-x, \{T_j\}_{j \geq 2})) \nu_1(dx) \right], \end{aligned}$$

since $\sum_{i=1}^{\infty} \mathbb{I}_{\Xi_{0i}}(x) = 1$. Finally,

$$\begin{aligned} &\mathbb{E} \left[\int_{T_1 \cap [0,1]^2} h(\tau(T_0-x | T_1-x, \{T_j\}_{j \geq 2})) \nu_1(dx) \right] \\ &= \mathbb{E}_{\{T_j\}_{j \geq 1}} \left[\int_{T_1 \cap [0,1]^2} \mathbb{E}_{T_0} [h(\tau(T_0-x | T_1-x, \{T_j\}_{j \geq 2}))] \nu_1(dx) \right] \\ &= \mathbb{E}_{\{T_j\}_{j \geq 1}} \left[\int_{T_1 \cap [0,1]^2} \mathbb{E}_{T_0} [h(\tau(T_0 | T_1-x, \{T_j\}_{j \geq 2}))] \nu_1(dx) \right] \\ &= \mathbb{E}_{T_0, \{T_j\}_{j \geq 2}} \mathbb{E}_{T_1} \left[\int_{T_1 \cap [0,1]^2} h(\tau(T_0 | T_1-x, \{T_j\}_{j \geq 2})) \nu_1(dx) \right] \\ &= \gamma_1 \mathbb{E} [h(\tau(T_0 | T_1^*, \{T_j\}_{j \geq 2}))], \end{aligned}$$

where the last equality is obtained from (III.2), replacing T and T^* by T_1 and T_1^* , respectively. Thus, (III.4) is proved. ■

Note that the random tessellations $\tau(T_0^* | T_1, T_2, \dots)$ and $\tau(T_0 | T_1^*, T_2, T_3, \dots)$ occurring in (III.3) can be considered as conditional versions of T^* under the condition that the origin belongs to an edge of the initial tessellation resp. the component tessellations, which occur with the probability γ_0/γ resp. γ_1/γ .

B. Simulation algorithm

The representation formula (III.3) for T^* derived in Theorem 3.1 enables us to simulate T^* if both T_0 and T_1 as well as their Palm versions T_0^* and T_1^* can be simulated. If T_j for $j = 0, 1$ is a PVT, PLT or PDT, respectively, then the simulation of T_j is straightforward and simulation algorithms for T_j^* are also available [12], [19], [20]. Moreover, (III.3) and the remark at the end of Section III-A yield a simulation algorithm for the Palm version X^* of the stationary Cox process X , which consists of the following main steps.

- 1) Simulate $U \sim U[0, 1]$. If $U < \gamma_0/\gamma$, go to step 2, else go to step 3.
- 2) Simulate T_0^* and subdivide the cells $\Xi_{01}^*, \Xi_{02}^*, \dots$ of T_0^* by T_1, T_2, \dots , respectively, which gives T^* .
- 3) Simulate T_0 , subdivide the zero cell Ξ_{01} of T_0 by T_1^* and subdivide the cells $\Xi_{02}, \Xi_{03}, \dots$ of T_0 by T_2, T_3, \dots , which gives T^* .
- 4) Construct $X^* = \{o\}$.
- 5) For $k = 1, 2, \dots$, generate $N_k \sim \text{Poi}(\lambda_\ell \nu_1(S_k))$, where S_k denotes the k th segment of ∂T^* ; if $N_k = n_k$, generate n_k points X_{k1}, \dots, X_{kn_k} , which are conditionally independent and uniformly distributed on S_k ; add the points X_{k1}, \dots, X_{kn_k} to X^* .

From a practical point of view, we always want to simulate X^* in a given (bounded) sampling window $W \subset \mathbb{R}^2$. Then, in many cases, it is reasonable to simulate T_0 and T_1 as well as T_0^* and T_1^* radially, where we have to choose appropriate stopping criteria depending on the type of the tessellations T_0 and T_1 . This kind of algorithm has many applications in the analysis and planning of (wired and wireless) telecommunication networks. For instance, it can be used in order to simulate the typical cell Ξ^* of the Voronoi tessellation induced by X , where we merely have to construct the Voronoi cell at o with respect to X^* . Furthermore, various distance distributions in such networks can be estimated based on samples of the typical cell Ξ^* , see e.g. [11], [12], [16] and Section IV.

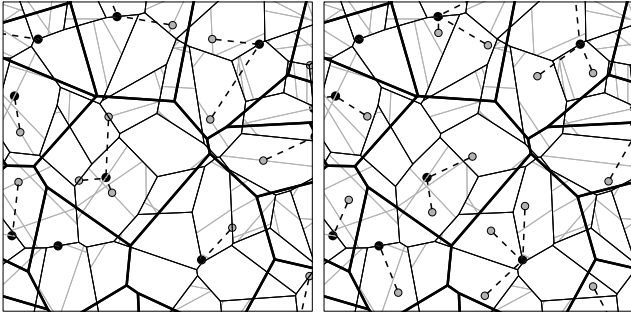


Fig. 2. Realizations of T, H and L together with the connection distances

IV. NUMERICAL RESULTS AND APPLICATIONS

We now focus on the case of an iterated tessellation $T = \tau(T_0 | T_1, T_2, \dots)$, where T_0 is a PVT and T_1, T_2, \dots are PLT. Note that other nestings based on PVT, PDT and PLT, respectively, can be analyzed similarly.

A. Typical Voronoi cell of Cox processes

The locations of network components in hierarchical telecommunication networks are often modeled by two stationary point processes $H = \{H_n\}$ and $L = \{L_n\}$ in \mathbb{R}^2 , where H represents the locations of high-level components and L represents the locations of low-level components. Suppose that each point of L is connected to its nearest point of H , i.e., a point L_n of L is connected to the point H_{k_n} of H if L_n is located in the Voronoi cell of H_{k_n} , see [4], [15]. The Voronoi cell of H_{k_n} is then called the serving zone of the high-level component located at this point. Thus the typical Voronoi cell of H is an important object in the global analysis and planning of telecommunication networks, see also Section III. Furthermore, samples of the typical Voronoi cell can be used in order to estimate the density of typical connection distances in hierarchical telecommunication networks, see Section IV-B.

Assume that H is a Cox process on the edge set of a PVT/PLT nesting. In order to determine distributional properties of the typical Voronoi cell of H , we simulated the Palm version H^* of H for different values of κ , γ_0 and γ_1 with $\gamma_0 + \gamma_1 = 1$. Based on these samples, we then computed the distribution of cell characteristics like perimeter and area. The results are displayed in Fig. 3. As one can see, we can move from PVT towards PLT if γ_0 decreases and hence γ_1 increases. Thus, we can interpolate between the distributions of the typical cell of the extremal cases where T is a PVT and PLT, respectively, by choosing PVT/PLT nestings for values of γ_0 from 1 to 0.

B. Distribution of connection distances

In [12] estimators for the density and distribution function of the typical (Euclidean) connection distance D^* from the typical point of L to its nearest point of H have been introduced for two different scenarios. Note that the distribution of D^* is formally defined via Palm distributions, but again it can be regarded as the limit of the empirical distributions of the Euclidean connection distances from all points of L

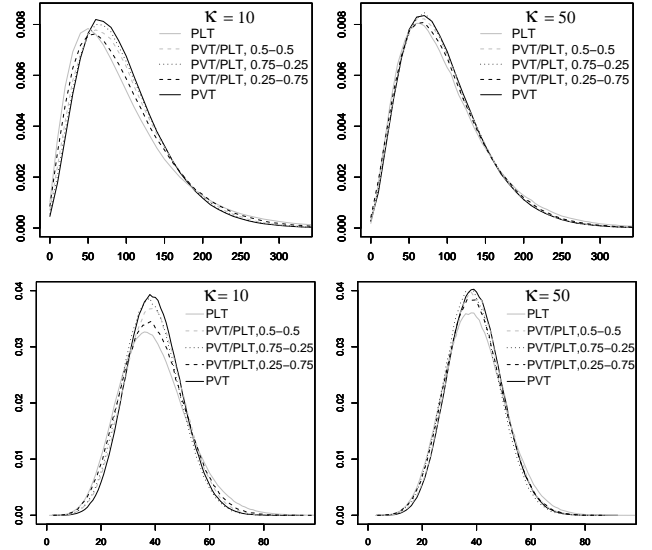


Fig. 3. Histograms for area (top) and perimeter (bottom) of the typical cell

in a family of unboundedly increasing sampling windows. Thus, the distribution of D^* is also an important object in the global analysis and planning of telecommunication networks. In both scenarios considered in [12], H is a Cox process on T , whereas L is either a planar Poisson process independent of H or a Cox process on the same tessellation T which is conditionally independent of H given T . Then, in both cases, estimators for the density and distribution function of D^* can be constructed based on samples of the typical Voronoi cell of H .

Let H be a Cox process on T with intensity $\lambda = \lambda_\ell \gamma$. If L is a planar Poisson process, then

$$\hat{f}_{D^*}(x; n) = \frac{\lambda_\ell \gamma}{n} \sum_{i=1}^n \nu_1(\Xi_i^* \cap \partial B(o, x)) \quad (IV.5)$$

can be used to estimate the probability density of D^* . Here Ξ_1^*, \dots, Ξ_n^* is an i.i.d. sample of the typical Voronoi cell of H and $\nu_1(\Xi_i^* \cap \partial B(o, x))$ denotes the intersection length of the circle $\partial B(o, x)$ with radius x centered at o inside Ξ_i^* . If L is a Cox process on T , then an estimator $\hat{F}_{D^*}(x; n)$ for the distribution function $F_{D^*}(x)$ is given by

$$\hat{F}_{D^*}(x; n) = \frac{\lambda_\ell}{n} \sum_{i=1}^n \nu_1(S_i^* \cap B(o, x)), \quad (IV.6)$$

where S_1^*, \dots, S_n^* denotes an i.i.d. sample of segment systems of the underlying tessellation T^* inside Ξ_1^*, \dots, Ξ_n^* , respectively. Based on \hat{F}_{D^*} we can then get an estimator \hat{f}_{D^*} for the density of D^* by computing difference quotients. The numerical results obtained from simulations of the typical cell of the Cox processes H are displayed in Fig. 4.

We again see that the distributions of D^* for PVT and PLT occur as extremal cases and that we can move from PVT to PLT if γ_0 goes from 1 to 0. Thus, considering a more flexible class of (iterated) tessellations, we now are in a position to arrive at a more flexible class of different distance distributions. This extension is useful in applications to real networks, whereas, so far, we were only able to use simpler (non-iterated) tessellation models.

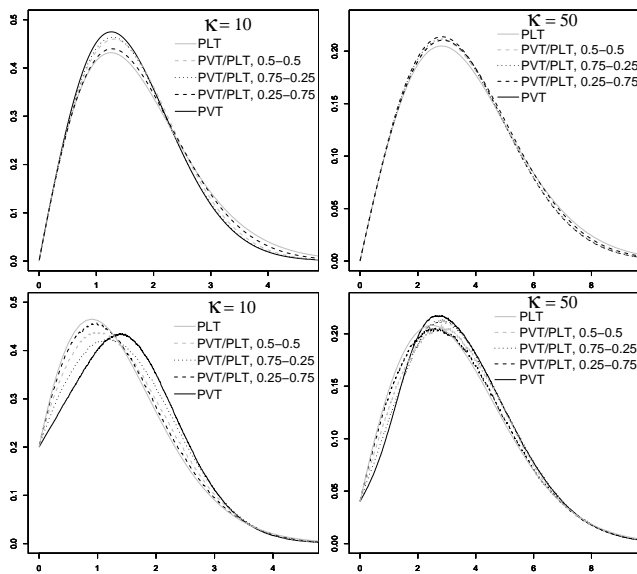


Fig. 4. Density of D^* if L is a Poisson process (top) or Cox process (bottom)

V. CONCLUSIONS

We investigate the Palm version X^* of stationary Cox processes X on iterated random tessellations T . In particular, we derive a representation formula for the Palm version T^* of T which includes the initial tessellation T_0 and the component tessellation T_1 of T as well as their Palm versions T_0^* and T_1^* . Using this formula, we are able to construct a simulation algorithm for X^* if both T_0, T_1 and their Palm versions T_0^*, T_1^* can be simulated.

Since simulation algorithms for PVT, PLT and PDT and their Palm version are available, we are now able to simulate the Palm version of Cox processes on iterated tessellations based on these three basic tessellation models. The new simulation algorithm can be used in the analysis of telecommunication networks. Based on simulations of X^* we can estimate the distributions of direct connection distances for wireless network models and the distributions of connection distances along the underlying street systems for access network models. This is an important extension of our earlier work since we can now use iterated tessellations as street models which are more flexible than the simpler (non-iterated) tessellation models PVT, PLT and PDT considered so far.

ACKNOWLEDGEMENT

This research has been supported by Orange Labs (Research agreement 46143714).

REFERENCES

- [1] E. Gilbert, "Random plane networks," *Journal of the Society of Industrial and Applied Mathematics*, vol. 9, pp. 533–543, 1961.
- [2] K.K. Leng, W.A. Massey, and W. Whitt, "Traffic models for wireless communication networks," *IEEE Journal on Selected Areas in Communications*, vol.12, pp. 1353–1364, 1994.
- [3] S. Foss and S. Zuyev, "On a certain Voronoi aggregative process related to a bivariate Poisson process," *Advances in Applied Probability*, vol. 28, pp. 965–981, 1996.
- [4] F. Baccelli, M. Klein, M. Lebourges, and S. Zuyev, "Stochastic geometry and architecture of communication networks," *Telecommunication Systems*, vol. 7, pp. 209–227, 1997.

- [5] F. Baccelli and S. Zuyev, "Poisson-Voronoi spanning trees with applications to the optimization of communication networks," *Operations Research*, vol. 47, pp. 619–631, 1999.
- [6] P. Gupta and P.R. Kumar, "The capacity of wireless networks," *IEEE Transactions on Information Theory*, vol. 46, pp. 388–404, 2000.
- [7] F. Baccelli and B. Blaszczyzyn, "Spatial Modeling of Wireless Communications, A Stochastic Geometry Approach. Foundations and Trends in Communications", NOW Publisher, 2009 (to appear).
- [8] M. Haenggi, J. G. Andrews, F. Baccelli, O. Dousse, and M. Franceschetti, "Stochastic geometry and random graphs for the analysis and design of wireless networks," *IEEE Journal on Selected Areas in Communications (to appear)*, 2009.
- [9] S. Zuyev, "Stochastic geometry and telecommunications networks," in: *Stochastic Geometry: Highlights, Interactions and New Perspectives*, W.S. Kendall and I. Molchanov, Eds., Oxford University Press (to appear), 2009.
- [10] C. Gloaguen, F. Fleischer, H. Schmidt, and V. Schmidt, "Analysis of shortest paths and subscriber line lengths in telecommunication access networks," *Networks and Spatial Economics (to appear)*, 2009.
- [11] C. Gloaguen, F. Voss, and V. Schmidt, "Parametric distance distributions for fixed access network analysis and planning," *Preprint (submitted)*, 2009.
- [12] F. Voss, C. Gloaguen, F. Fleischer, and V. Schmidt, "Distributional properties of Euclidean distances in wireless networks involving road systems," *IEEE Journal on Selected Areas in Communications (to appear)*, 2009.
- [13] F. Voss, C. Gloaguen, and V. Schmidt, "Capacity distributions in spatial stochastic models for telecommunication networks," *Proceedings of the 10th European Congress of Stereology and Image Analysis*, Milan, June 2009.
- [14] C. Gloaguen, F. Fleischer, H. Schmidt, and V. Schmidt, "Fitting of stochastic telecommunication network models, via distance measures and Monte-Carlo tests," *Telecommunication Systems*, vol. 31, pp. 353–377, 2006.
- [15] C. Gloaguen, H. Schmidt, R. Thiedmann, J. P. Lanquetin, and V. Schmidt, "Comparison of network trees in deterministic and random settings using different connection rules," in *Proceedings of the 3rd Workshop on Spatial Stochastic Models for Wireless Networks (SpaSWiN)*, Limassol, April 2007.
- [16] F. Voss, C. Gloaguen, F. Fleischer, and V. Schmidt, "Density estimation of typical shortest path lengths in telecommunication networks," *Preprint*, 2009.
- [17] R. Maier and V. Schmidt, "Stationary iterated random tessellations," *Advances in Applied Probability*, vol. 35, pp. 337–353, 2003.
- [18] R. Maier, J. Mayer, and V. Schmidt, "Distributional properties of the typical cell of stationary iterated tessellations," *Mathematical Methods of Operations Research*, vol. 59, pp. 287–302, 2004.
- [19] C. Gloaguen, F. Fleischer, H. Schmidt, and V. Schmidt, "Simulation of typical Cox-Voronoi cells, with a special regard to implementation tests," *Mathematical Methods of Operations Research*, vol. 62, pp. 357–373, 2005.
- [20] F. Fleischer, C. Gloaguen, V. Schmidt, and F. Voss, "Simulation of the typical Poisson-Voronoi-Cox-Voronoi cell," *Journal of Statistical Computation and Simulation (to appear)*, 2009.
- [21] F. Fleischer, C. Gloaguen, H. Schmidt, V. Schmidt, and F. Schweiggert, "Simulation algorithm of typical modulated Poisson-Voronoi cells and application to telecommunication network modelling," *Japan Journal of Industrial and Applied Mathematics*, vol. 25, pp. 305–330, 2008.
- [22] D. Daley and D. Vere-Jones, *An Introduction to the Theory of Point Processes*. New York: Springer, 2003/08, vol. I/II.
- [23] A. Okabe, B. Boots, K. Sugihara, and S. N. Chiu, *Spatial Tessellations*, 2nd ed. Chichester: J. Wiley & Sons, 2000.
- [24] R. Schneider and W. Weil, *Stochastic and Integral Geometry*. Berlin: Springer, 2008.
- [25] D. Stoyan, W. S. Kendall, and J. Mecke, *Stochastic Geometry and its Applications*, 2nd ed. Chichester: J. Wiley & Sons, 1995.